

1                   **Boosting of SARS-CoV-2 immunity in nonhuman primates using**  
2   **an oral rhabdoviral vaccine**

3 Kah-Whye Peng<sup>1,2,3</sup>, Timothy Carey<sup>2</sup>, Patrycja Lech<sup>2</sup>, Rianna Vandergaast<sup>2</sup>, Miguel Á. Muñoz-  
4 Alía<sup>3</sup>, Nandakumar Packiriswamy<sup>3</sup>, Clement Gnanadurai<sup>2</sup>, Karina Krotova<sup>2</sup>, Mulu Tesfay<sup>2</sup>,  
5 Christopher Ziegler<sup>2</sup>, Michelle Haselton<sup>2</sup>, Kara Sevola<sup>2</sup>, Chase Lathrum<sup>2</sup>, Samantha Reiter<sup>2</sup>, Riya  
6 Narjari<sup>2</sup>, Baskar Balakrishnan<sup>3</sup>, Lukkana Suksanpaisan<sup>2</sup>, Toshie Sakuma<sup>1</sup>, Jordan Recker<sup>1</sup>,  
7 Lianwen Zhang<sup>3</sup>, Scott Waniger<sup>1</sup>, Luke Russell<sup>1</sup>, Christopher D. Petro<sup>4</sup>, Christos A. Kyratsous<sup>4</sup>,  
8 Alina Baum<sup>4</sup>, Jody L. Janecek<sup>5</sup>, Rachael M. Lee<sup>5</sup>, Sabarinathan Ramachandran<sup>5</sup>, Melanie L.  
9 Graham<sup>5</sup>, Stephen J. Russell<sup>1,2,3\*</sup>

10  
11 <sup>1</sup>Vyriad Inc, Rochester MN 55901, USA,

12 <sup>2</sup>Imanis Life Sciences, Rochester MN 55901, USA,

13 <sup>3</sup>Department of Molecular Medicine, Mayo Clinic, MN 55905, USA,

14 <sup>4</sup>Regeneron Pharmaceuticals Inc, Tarrytown, NY 10591, USA,

15 <sup>5</sup>Department of Surgery, University of Minnesota, USA

16 Corresponding author. Email: [sjrussell@vyriad.com](mailto:sjrussell@vyriad.com)

17

18

19 **Abstract**

20 An orally active vaccine capable of boosting SARS-CoV-2 immune responses in previously  
21 infected or vaccinated individuals would help efforts to achieve and sustain herd immunity.  
22 Unlike mRNA-loaded lipid nanoparticles and recombinant replication-defective adenoviruses,  
23 replicating vesicular stomatitis viruses with SARS-CoV-2 spike glycoproteins (VSV-SARS2)  
24 were poorly immunogenic after intramuscular administration in clinical trials. Here, by G protein  
25 trans-complementation, we generated VSV-SARS2(+G) virions with expanded target cell  
26 tropism. Compared to parental VSV-SARS2, G-supplemented viruses were orally active in  
27 virus-naïve and vaccine-primed cynomolgus macaques, powerfully boosting SARS-CoV-2  
28 neutralizing antibody titers. Clinical testing of this oral VSV-SARS2(+G) vaccine is planned.

29

30 **Keywords:** SARS-CoV-2, oral vaccine, rhabdovirus, VSV, neutralizing antibodies, T cells

31

## 32 **Introduction**

33 Control of the SARS-CoV-2 pandemic will depend in part upon the global deployment of  
34 effective vaccines [1]. However, all currently approved SARS-CoV-2 vaccines are administered  
35 via intramuscular injection which increases the cost and complexity of vaccination programs,  
36 contributes to vaccine hesitancy and fails to stimulate mucosal immunity [2, 3]. Also, protective  
37 antibody titers are known to wane after successful vaccination (or after natural infection), such  
38 that periodic booster immunizations will be needed to sustain immunity, particularly in  
39 vulnerable individuals, so long as the virus remains endemic in the human population [4-6].

40  
41 Since oral and nasal mucosal surfaces are the primary portal of entry for SARS-like  
42 coronaviruses, the induction of mucosal immunity (via secretory IgA) may be the best way to  
43 prevent the virus from ever getting a foothold in the upper airways, thereby eliminating the risk  
44 of asymptomatic infection and virus shedding in vaccinated individuals which could aid virus  
45 transmission [7]. Available data from previous studies suggests that mucosal protection can be  
46 achieved most readily via mucosal vaccination using an oral or intranasal delivery route [3]  
47 which has been exemplified in previously licensed vaccines (e.g. Rotarix® and oral polio  
48 vaccines). From a cost, convenience and simplicity perspective, the oral route is preferred over  
49 the intranasal route since it does not require the use of a specialized delivery device (e.g.  
50 nebulizer). Also, from a safety perspective oral delivery avoids the risk that a live viral vaccine  
51 administered intranasally might spread into the brain via the olfactory neurons which pass  
52 through the cribriform plate at the apex of the nasal cavity [8]. Finally, compared to available  
53 injectable vaccines, oral vaccines are much preferred by children and adolescents whose high  
54 prevalence of vaccine hesitancy is linked to fear of needles [2, 9].

55

56 Here, to develop an orally active viral vaccine capable of expressing the immunogenic SARS-  
57 CoV-2 spike glycoprotein in oral mucosa, we exploited the known tropism of vesicular stomatitis  
58 virus (VSV). Vesicular stomatitis is a self-limited illness of cattle and other ungulate species  
59 characterized by blistering of the oral mucosa and hooves [10]. The disease is endemic in Central  
60 America and the Southern United States, and the causative agent is vesicular stomatitis virus  
61 (VSV), a mosquito borne Vesiculovirus belonging to the family Rhabdoviridae. Human  
62 exposures to VSV infected cattle lead to asymptomatic seroconversion or sometimes a brief  
63 febrile illness with associated oral blistering [10]. VSV seroprevalence is very low in the human  
64 population, even in endemic areas [11]. VSV is a bullet-shaped virus with a lipid envelope and a  
65 single stranded negative sense RNA genome of approximately 11kb, comprising five genes  
66 encoding nucleocapsid (N), phosphoprotein (P), matrix (M), glycoprotein (G) and polymerase  
67 (L) proteins. Virus entry is mediated via the interaction of the viral G protein with the low  
68 density lipoprotein (LDL) receptor, ubiquitously expressed on mammalian cells [12].

69  
70 To generate an orally active VSV-SARS2(+G) vaccine we substituted the G cistron of an Indiana  
71 strain VSV genome with a codon-optimized sequence encoding the Wuhan strain SARS-CoV-2  
72 spike glycoprotein (S) and amplified the recombinant virus on Vero cells transiently expressing  
73 the G protein (Fig. 1A). To facilitate S protein incorporation and G-independent propagation of  
74 the recombinant VSV-SARS2 viruses, a 19 amino acid S protein cytoplasmic tail truncation was  
75 introduced into the S protein [13]. The virus rescued from this construct was able to propagate  
76 autonomously, albeit slowly, with characteristic syncytial cytopathic effect on A549 cells  
77 transduced with the ACE2 receptor, but not on parental A549 cells (Fig. 1B). Autonomously  
78 replicating non-G-deleted VSVs encoding the SARS-CoV2 spike protein that were generated in

79 parallel were found to replicate efficiently on ACE2 negative cells, but rapidly lost expression of  
80 the spike protein, primarily via point mutations in key upstream regulatory sequences (data not  
81 shown). The stably and autonomously replicating VSV-SARS2 virions were next propagated on  
82 ACE2 receptor positive Vero cells transfected with a VSV-G expression plasmid to trans-  
83 pseudotype them with the G protein, which is also known to drive more efficient virus budding  
84 [14]. G-protein incorporation led to an approximately 10-fold enhancement of the infectious  
85 titer of the VSV-SARS2(+G) virus preparations (titers of  $2 \times 10^9$  TCID<sub>50</sub> per ml were achieved  
86 for the G supplemented viruses versus maximum titer of  $5.1 \times 10^7$  TCID<sub>50</sub> without G protein. In  
87 a parallel study, incorporating the SARS-CoV-2 spike coding sequences as an additional cistron  
88 (that is, without deletion of G) proved to be highly unstable since their replication was not  
89 dependent on the integrity of the SARS-CoV-2 spike.

90  
91 Biochemical characterization of the recombinant virus particles confirmed the incorporation a  
92 partially cleaved S protein in pure VSV-SARS2 virions, and the co-incorporation of S and G  
93 proteins in the G-pseudotyped VSV-SARS2(+G) virions (Fig. 1C). SARS-CoV2 S protein  
94 expression after infection with VSV-SARS2 or VSV-SARS2(+G) was confirmed by western  
95 blotting and/or flow cytometry of ACE2 negative baby hamster kidney cells (BHK) and ACE2  
96 positive Vero cells after infection by the respective viruses (Fig. 1C and D). VSV-SARS2 virions  
97 were neutralized by a cocktail of monoclonal anti-S SARS-CoV-2 neutralizing antibodies, but  
98 not by anti-G antibodies, indicating that they enter cells exclusively via their displayed S protein  
99 (Fig. 1E). In contrast, after treatment with anti-S or anti-G antibodies, G-pseudotyped VSV-  
100 SARS2(+G) virions retained 20% or 4% infectivity respectively but were more fully neutralized  
101 when the anti-S and anti-G antibodies were used in combination (Fig. 1E).

102

103 To facilitate in vivo studies in non-human primates (NHP), and possible clinical translation, mid-  
104 scale preparations of the VSV-SARS2 and VSV-SARS2(+G) viruses were generated using  
105 adherent GMP-qualified Vero cells as the substrate. Crude viral supernatants from these  
106 production runs were clarified by centrifugation and filtration, treated with benzonase, and  
107 purified by tangential flow filtration prior to cryopreservation. Viral stocks were titrated post-  
108 thawing by TCID<sub>50</sub> assay on Vero cell monolayers, then characterized for S and G protein  
109 incorporation and endotoxin content.

110

111 Expression of ACE2 receptors is not prominent on primate myocytes [14]. However, based on a  
112 published report demonstrating protective immunity to SARS-CoV-2 in hamsters vaccinated by  
113 intramuscular administration of a G-deficient VSV-ΔG-SARS-CoV-2 construct [15], we tested  
114 our own G-deficient VSV-SARS2 construct by intramuscular (IM, 10<sup>7</sup> TCID<sub>50</sub>) vaccination of  
115 six virus-naive cynomolgus macaques (Fig. 2A). Compared to unvaccinated control animals, all  
116 monkeys in this experimental group developed detectable anti-S antibody responses by 4 weeks  
117 after vaccination (Fig. 2, B, C). However, the absolute magnitude of the anti-spike IgG and  
118 neutralizing antibody titers observed in these animals were very low relative to mean human  
119 convalescent titers (Faracet. In parallel with this intramuscular study, 10 mls of the virus (10<sup>7</sup>  
120 TCID<sub>50</sub>) was administered into the oral cavity of animals (PO) under brief sedation. Immune  
121 responses to the oral application of the virus were not detected in any of the animals in this group  
122 (Fig. 2, B, C). The conclusion of this preliminary study in cynomolgus macaques was that the  
123 G-deficient VSV-SARS2 virus was weakly immunogenic when administered by the  
124 intramuscular route and is minimally immunogenic by the oral route.

125

126 To determine whether G protein supplementation could enhance the potency of the recombinant  
127 VSV vaccine, we administered VSV-SARS2(+G) to a total of four virus-naive cynomolgus  
128 macaques, either by IM injection (n=2) or PO (n=2). Both IM vaccinated animals and one of the  
129 orally vaccinated animals rapidly generated high IgG and neutralizing antibody titers against the  
130 SARS-CoV-2 spike glycoprotein (Fig. 3, A, B). Neutralizing antibody titers were well  
131 maintained with no significant decline in two of the three responding animals until the end of the  
132 study (six months post vaccination) indicating excellent durability of the immune response to  
133 this vaccine formulation. Interestingly, even though the VSV-SARS2(+G) virus does not encode  
134 the G protein, both IM-vaccinated animals generated low titers of G-reactive VSV neutralizing  
135 antibodies (Fig. 3C), indicating that even the small amount of G protein carried by the injected  
136 virus particles was sufficient to induce an immune response via this route. In contrast, anti-G  
137 antibodies were not detected in the orally vaccinated animals (Fig. 3C), indicating that particle-  
138 associated G protein may be less likely to provoke an immune response when the viruses are  
139 administered orally.

140

141 Analysis of T cell responses to the SARS-CoV-2 S protein in vaccinated macaques that  
142 seroconverted demonstrated an increase in spike antigen specific interferon gamma (IFN- $\gamma$ )  
143 ELISPOT positive T cells but not IL4 positive T cells, indicating Th<sub>1</sub> skewing (Fig. 3D). In light  
144 of the importance of this observation, we conducted confirmatory studies in immunized immune  
145 competent mice by intraperitoneal injection of the VSV-SARS2(+G) virus. As shown in  
146 supplemental figure 1, all vaccinated mice had a robust anti-spike antibody response with  
147 predominance of IgG2a antibodies compared to IgG1, further confirming the potent

148 immunogenicity of the platform with associated Th<sub>1</sub> skewing [16] of the immune response in the  
149 mouse model.

150

151 To determine whether the orally administered VSV-SARS2(+G) vaccine might have the ability  
152 to refresh and amplify the SARS-CoV-2 immune responses of individuals previously infected or  
153 vaccinated, but with low or waning titers of SARS-CoV-2 neutralizing antibodies, we orally  
154 boosted all six cynomolgus macaques from Experiment 1, Group A, 42 days after they received  
155 the intramuscular G-deficient VSV-SARS2 vaccine (Fig. 4A). Four animals received a high dose  
156 ( $10^9$  TCID<sub>50</sub>) of the oral vaccine and two animals received a low dose ( $5 \times 10^6$  TCID<sub>50</sub>).  
157 Logarithmic increases in the total IgG and neutralizing antibody titers were observed in all four  
158 animals in the high dose group within a week of receiving the oral boost (Fig. 4, B-D). Similar  
159 boosting of the antibody response was observed in one of the two animals in the low dose group  
160 (Fig. 4, B-D). Neutralizing antibody titers were concordant (fig. S2) between the vesiculovirus  
161 (Fig. 4C) and lentivirus pseudovirus assays (Fig. 4D). In addition, we have previously shown that  
162 the neutralizing antibody assay using the vesiculo-pseudovirus has good correlation ( $R=0.89$ ,  $p <$   
163  $0.0001$ ) with the classical plaque reduction neutralizing titer PRNT assay using the BSL3 live  
164 SARS-CoV-2 virus [17]. Analysis of peripheral blood mononuclear cells revealed significant  
165 increases in S protein specific IFN $\gamma$ -secreting T cells in these orally boosted animals, but not of  
166 IL4-secreting T cells in a ELISPOT assay (Fig. 4E). Significantly, anti-G antibodies were not  
167 detected in any of the orally boosted animals (Fig. 4F), suggesting that it may be possible to use  
168 the G-pseudotyped platform repeatedly in the same individual to boost immunity against diverse  
169 coronavirus spike glycoproteins. Analysis of buccal and bronchoalveolar lavage (BAL) fluid



170 obtained at euthanasia from these orally boosted and control animals revealed a substantial  
171 increase in the level of spike specific IgA as an indicator of mucosal immunity (Fig. 4, G and H).

172

173 The tolerability of VSV-SARS2 and VSV-SARS2(+G) vaccines was examined in all NHPs via  
174 physical examination, behavioral observations, complete blood counts, and serum chemistries,  
175 with a complete necropsy at the end of the study. Body weights were stable with a gain trend  
176 and there were no significant changes in the serum C-reactive protein, an acute inflammation  
177 marker (fig. S3). Mild increases in body temperature were observed within the normal range for  
178 vaccinated animals and were observed with equivalent frequency in sham-vaccinated animals. A  
179 low incidence of vomiting and inappetence was observed following sedation in both sham  
180 controls and vaccinated animals which is a well-known side effect of the drugs used for  
181 sedation. The vaccine delivery sites (oral and injection) of all test and control animals were  
182 examined regularly after virus exposure for evidence of irritation or inflammation. The only  
183 finding of note was in one animal that had transient and mild mucosal changes consistent with  
184 blistering, observed on the upper gingiva (2 x 4 mm) day 11 post vaccination with complete  
185 resolution at the next exam at day 21, and ulceration (4 mm) of the buccal mucosa day 35 post  
186 vaccination which resolved by day 56 and did not alter feeding habits or interfere with daily  
187 activities. Importantly, there was no infectious virus recovered from the saliva or buccal swabs  
188 from this animal, nor from any body fluids collected from any of the experimental animals  
189 (serum, buccal, nasal, rectal swabs) at any time point. Complete blood counts remained within  
190 normal limits throughout follow-up post vaccine administration and the renal and hepatic  
191 functional measurements did not indicate any adverse reaction to immunization which was  
192 confirmed by histology. Overall, there was minimal vaccine toxicity with oral administration of

193 the VSV-SARS2(+G) virus particles and the vaccine was well-tolerated in cynomolgus  
194 macaques.

195  
196 Overall, our data support the clinical advancement of VSV-SARS2(+G) for oral booster  
197 vaccination of individuals previously infected or vaccinated but who have low or rapidly waning  
198 antibody titers. Previous studies have shown that peak post-SARS-CoV-2 infection and post-  
199 vaccination neutralizing antibody titers to SARS-CoV-2 differ between individuals based on age,  
200 infection severity and vaccine identity [18]. Antibody titers have also been shown to fall quite  
201 rapidly over time with half-lives varying from 2.5 and 6 months, signifying 4-fold to 25-fold titer  
202 reductions in the first year [4, 6, 19]. Thus, while the appropriate timing of SARS-CoV-2  
203 vaccine booster shots has not yet been determined for specific subgroups of individuals, booster  
204 vaccination will likely be an important part of the strategy for longer-term control of the  
205 pandemic. Future studies comparing the efficacy of oral booster doses of VSV-SARS-CoV-2 and  
206 VSV-SARS2(G) in non-human primates would also be warranted after priming with currently  
207 approved vaccines.

208  
209 Compared to currently approved mRNA and adenoviral vaccines which are administered by  
210 intramuscular injection, mucosal vaccination may offer a more reliable and durable defense  
211 against SARS-CoV-2 infection [3]. Mucosal surfaces in the nose and mouth provide the primary  
212 portal of entry for respiratory pathogens such as SARS-CoV-2 and are best protected by  
213 secretory polymeric IgA in mucus and saliva. Secretory polymeric IgA is efficiently induced by  
214 mucosal vaccines because they interact directly with mucosal associated lymphoid tissues such  
215 as the lingual and palatine tonsils which encircle the posterior outlet of the oral cavity. Oral

216 mucosal vaccination may also overcome some of the logistical drawbacks of injectable vaccines  
217 such as the limited availability and high cost of vials, needles, syringes, and trained personnel,  
218 and the high prevalence of needle phobia in preadolescents, adolescents and college students.  
219 Comparing to intranasal vaccine delivery which has been successfully developed and deployed  
220 for influenza prevention [20], oral delivery may be a preferred approach to avoid the risks (and  
221 costs) of live virus aerosolization and CNS exposure associated with intranasal delivery.

222  
223 Interestingly, while it was generally accepted at the outset of the SARS-CoV-2 pandemic that  
224 protein, mRNA and nonreplicating adenoviral vaccines could be developed very rapidly, it was  
225 also argued that vaccines built on replicating viral platforms might prove to be more potent,  
226 potentially affording protection after a single dose. Based on the extraordinary success of VSV-  
227 EBOV, a G-substituted VSV encoding the Ebola surface glycoprotein, which fully protects  
228 against Ebola virus infection within 2 weeks after a single intramuscular shot [21], it was  
229 predicted that a G-substituted VSV encoding the SARS-CoV-2 spike glycoprotein would be  
230 equally effective as an intramuscular vaccine to protect against COVID-19. However, in human  
231 trials the efficacy of this G-substituted construct, administered by intramuscular injection, fell  
232 short of expectations and induced suboptimal titers of neutralizing antibodies [22]. Our studies in  
233 cynomolgus macaques confirm the low immunogenicity of the VSV-SARS2 vaccine construct,  
234 but further extend the narrative by demonstrating the enormous promise of the same construct as  
235 an oral mucosal booster vaccine when modified to incorporate the VSV.G protein. We have  
236 therefore recently engineered a series of VSV-SARS2 constructs encoding the spike proteins of  
237 emerging SARS-CoV-2 variants. G protein pseudotyping of a replication defective VSV  
238 encoding the SARS-CoV spike glycoprotein was shown previously to enhance the

239 immunogenicity of the construct when administered to NHPs by IM injection, but oral  
240 administration was not attempted [23]. Interestingly, another group recently exploited G protein  
241 trans-complementation as a way to restore the immunogenicity of a G-deleted VSV-derived  
242 vaccine for SARS-CoV-2 in ACE2 receptor negative mice [24]. VSV-eGFP-SARS-CoV-2, an  
243 autonomously replicating ACE2 receptor-dependent VSV which encodes the SARS2 spike  
244 glycoprotein and a GFP reporter gene was trans-complemented with “a small amount” of VSV-G  
245 protein, then used to vaccinate mice via the intraperitoneal route which resulted in robust,  
246 protective anti-spike antibody responses. These investigators further demonstrated the feasibility  
247 of intranasal vaccination using the same construct, but without G protein supplementation, in  
248 mice that were transgenic for the ACE2 receptor [24]. Although not formally proven, we  
249 speculate that the superior immunogenicity of the G-supplemented virus preparation, both by IM  
250 and PO routes, reflects a higher efficiency of muscle cell and oral mucosal transduction due the  
251 virus-displayed G protein interacting with the LDL receptor on myocytes and oral mucosal  
252 epithelium. We further speculate that the high potency of the intramuscular VSV-EBOV vaccine  
253 is likely the consequence of a high abundance of Ebola virus receptors in muscle tissue leading  
254 to efficient transduction by the injected viral particles, and that conversely the inferior efficacy of  
255 the VSV-SARS2 vaccine in the absence of G protein supplementation, is the consequence of low  
256 muscle expression of ACE2, the primary receptor for the SARS-CoV-2 spike protein [14, 25].  
257 However, we cannot rule out the possibility of an additional contribution due to an immune  
258 adjuvant effect of the G protein itself.

259

260 The absence of an immune response to the VSV G protein when the G-supplemented viruses  
261 were administered orally is an important feature of the VSV-SARS2(+G) system which will

262 allow for the future generation and deployment of G-supplemented VSVs whose G cistron has  
263 been substituted for envelope glycoproteins from other coronaviruses (e.g. those causing the  
264 common cold), or from pathogenic viruses belonging to non-coronaviridae families. G-  
265 supplemented VSV particles may therefore eventually prove to be a versatile oral mucosal  
266 vaccine platform capable of addressing a range of respiratory pathogens.

267  
268 In summary, as a proof of concept, we utilized a relevant translational NHP model to  
269 demonstrate the safety and oral immunogenicity of a VSV-derived mucosal vaccine for SARS-  
270 CoV-2. Since completing these studies, we have developed a process for the scaled (GMP)  
271 manufacture of VSV-SARS-2(+G) in 293 suspension cultures and we have demonstrated product  
272 stability for up to 2 weeks at 4°C. Pre-IND discussions with FDA are ongoing.

273

## 274 REFERENCES

- 275 [1] Wouters OJ, Shadlen KC, Salcher-Konrad M, Pollard AJ, Larson HJ, Teerawattananon Y, et al.  
276 Challenges in ensuring global access to COVID-19 vaccines: production, affordability, allocation, and  
277 deployment. *Lancet*. 2021;397:1023-34.
- 278 [2] Ryan KA, Filipp SL, Gurka MJ, Zirulnik A, Thompson LA. Understanding influenza vaccine perspectives  
279 and hesitancy in university students to promote increased vaccine uptake. *Heliyon*. 2019;5:e02604.
- 280 [3] Mudgal R, Nehul S, Tomar S. Prospects for mucosal vaccine: shutting the door on SARS-CoV-2. *Hum*  
281 *Vaccin Immunother*. 2020;16:2921-31.
- 282 [4] Vandergaast R, Carey T, Reiter S, Lathrum C, Lech P, Gnanadurai C, et al. IMMUNO-COV™ v2.0:  
283 Development and Validation of a High-Throughput Clinical Assay for Measuring SARS-CoV-2-Neutralizing  
284 Antibody Titers. *medRxiv*. 2021:2021.02.16.21251653.
- 285 [5] Tan Y, Liu F, Xu X, Ling Y, Huang W, Zhu Z, et al. Durability of neutralizing antibodies and T-cell  
286 response post SARS-CoV-2 infection. *Front Med*. 2020;14:746-51.
- 287 [6] Widge AT, Roupael NG, Jackson LA, Anderson EJ, Roberts PC, Makhene M, et al. Durability of  
288 Responses after SARS-CoV-2 mRNA-1273 Vaccination. *N Engl J Med*. 2021;384:80-2.
- 289 [7] Travis CR. As Plain as the Nose on Your Face: The Case for A Nasal (Mucosal) Route of Vaccine  
290 Administration for Covid-19 Disease Prevention. *Front Immunol*. 2020;11:591897.
- 291 [8] Durrant DM, Ghosh S, Klein RS. The Olfactory Bulb: An Immunosensory Effector Organ during  
292 Neurotropic Viral Infections. *ACS Chem Neurosci*. 2016;7:464-9.
- 293 [9] Baxter AL, Cohen LL, Burton M, Mohammed A, Lawson ML. The number of injected same-day  
294 preschool vaccines relates to preadolescent needle fear and HPV uptake. *Vaccine*. 2017;35:4213-9.
- 295 [10] Letchworth GJ, Rodriguez LL, Del carrera J. Vesicular stomatitis. *Vet J*. 1999;157:239-60.

- 296 [11] Roberts A, Buonocore L, Price R, Forman J, Rose JK. Attenuated vesicular stomatitis viruses as  
297 vaccine vectors. *J Virol.* 1999;73:3723-32.
- 298 [12] Finkelshtein D, Werman A, Novick D, Barak S, Rubinstein M. LDL receptor and its family members  
299 serve as the cellular receptors for vesicular stomatitis virus. *Proc Natl Acad Sci U S A.* 2013;110:7306-11.
- 300 [13] Fukushi S, Watanabe R, Taguchi F. Pseudotyped vesicular stomatitis virus for analysis of virus entry  
301 mediated by SARS coronavirus spike proteins. *Methods Mol Biol.* 2008;454:331-8.
- 302 [14] Hamming I, Timens W, Bulthuis ML, Lely AT, Navis G, van Goor H. Tissue distribution of ACE2  
303 protein, the functional receptor for SARS coronavirus. A first step in understanding SARS pathogenesis. *J*  
304 *Pathol.* 2004;203:631-7.
- 305 [15] Yahalom-Ronen Y, Tamir H, Melamed S, Politi B, Shifman O, Achdout H, et al. A single dose of  
306 recombinant VSV-G-spike vaccine provides protection against SARS-CoV-2 challenge. *Nat Commun.*  
307 2020;11:6402.
- 308 [16] Stevens TL, Bossie A, Sanders VM, Fernandez-Botran R, Coffman RL, Mosmann TR, et al. Regulation  
309 of antibody isotype secretion by subsets of antigen-specific helper T cells. *Nature.* 1988;334:255-8.
- 310 [17] Vandergaast R, Carey T, Reiter S, Lech P, Gnanadurai C, Tesfay M, et al. Development and validation  
311 of IMMUNO-COV: a high-throughput clinical assay for detecting antibodies that neutralize SARS-CoV-2.  
312 *bioRxiv.* 2020.
- 313 [18] Earle KA, Ambrosino DM, Fiore-Gartland A, Goldblatt D, Gilbert PB, Siber GR, et al. Evidence for  
314 antibody as a protective correlate for COVID-19 vaccines. *medRxiv.* 2021:2021.03.17.20200246.
- 315 [19] Lau EHY, Tsang OTY, Hui DSC, Kwan MYW, Chan WH, Chiu SS, et al. Neutralizing antibody titres in  
316 SARS-CoV-2 infections. *Nat Commun.* 2021;12:63.
- 317 [20] Carter NJ, Curran MP. Live attenuated influenza vaccine (FluMist(R); Fluenz): a review of its use in  
318 the prevention of seasonal influenza in children and adults. *Drugs.* 2011;71:1591-622.
- 319 [21] Suder E, Furuyama W, Feldmann H, Marzi A, de Wit E. The vesicular stomatitis virus-based Ebola  
320 virus vaccine: From concept to clinical trials. *Hum Vaccin Immunother.* 2018;14:2107-13.
- 321 [22] Herper M, Branswell H. In a major setback, Merck to stop developing its two Covid-19 vaccines and  
322 focus on therapies. 2021.
- 323 [23] Kapadia SU, Simon ID, Rose JK. SARS vaccine based on a replication-defective recombinant vesicular  
324 stomatitis virus is more potent than one based on a replication-competent vector. *Virology.*  
325 2008;376:165-72.
- 326 [24] Case JB, Rothlauf PW, Chen RE, Kafai NM, Fox JM, Smith BK, et al. Replication-Competent Vesicular  
327 Stomatitis Virus Vaccine Vector Protects against SARS-CoV-2-Mediated Pathogenesis in Mice. *Cell Host*  
328 *Microbe.* 2020;28:465-74 e4.
- 329 [25] Zhou P, Yang X-L, Wang X-G, Hu B, Zhang L, Zhang W, et al. A pneumonia outbreak associated with a  
330 new coronavirus of probable bat origin. *Nature.* 2020;579:270-3.
- 331 [26] Ammayappan A, Nace R, Peng K-W, Russell SJ. Neuroattenuation of Vesicular Stomatitis Virus  
332 through Picornaviral Internal Ribosome Entry Sites. *Journal of Virology.* 2013;87:3217-28.
- 333 [27] Lefrancois L, Lyles DS. The interaction of antibody with the major surface glycoprotein of vesicular  
334 stomatitis virus. I. Analysis of neutralizing epitopes with monoclonal antibodies. *Virology.* 1982;121:157-  
335 67.
- 336 [28] I.f.L.A.R. Guide for the Care and Use of Laboratory Animals. Guide for the Care and Use of  
337 Laboratory Animals. Washington (DC)2011.
- 338 [29] Graham ML. Positive Reinforcement Training and Research. In: Shapiro SJ, editor. Handbook of  
339 Primate Behavioral Management Boca Raton: CRC Press; 2017. p. 185-200.
- 340 [30] Graham ML, Rieke EF, Mutch LA, Zolondek EK, Faig AW, Dufour TA, et al. Successful implementation  
341 of cooperative handling eliminates the need for restraint in a complex non-human primate disease  
342 model. *J Med Primatol.* 2012;41:89-106.

343 [31] Mrkic B, Pavlovic J, Rulicke T, Volpe P, Buchholz CJ, Hourcade D, et al. Measles virus spread and  
344 pathogenesis in genetically modified mice. *J Virol.* 1998;72:7420-7.  
345 [32] Crawford KHD, Eguia R, Dingens AS, Loes AN, Malone KD, Wolf CR, et al. Protocol and Reagents for  
346 Pseudotyping Lentiviral Particles with SARS-CoV-2 Spike Protein for Neutralization Assays. *Viruses.*  
347 2020;12.  
348

## 349 **ACKNOWLEDGEMENTS**

350 We gratefully acknowledge the excellent and expert contributions of Carlen Hill, Jody Janecek,  
351 Ruby Klish, Rachael Lee, Christian Moses, Brenna Mulhollam, Lucas Mutch, Melanie  
352 Niewinski, Sierra Palmer, Scott Oppler, Jordan Truell for husbandry and clinical care of our  
353 animals, Mikayla Chavis, Sarah Gresch, Laura Hocum Stone for in vitro studies, Meghan Moore  
354 and Timothy O'Brien for pathology, and Mellani Lubaug, Margret Tavai-Tuisalo'o, Jade Wilder  
355 for administrative support at the University of Minnesota's Preclinical Research Center. We  
356 gratefully acknowledge the excellent and expert support of Parthasarathy Rangarajan, Naoya  
357 Sato, Anna Tran, Ravi Maisuria, Amar Singh, and Janice Anoka for sample processing and  
358 specimen archiving.

359

## 360 **AUTHOR CONTRIBUTIONS**

361 SJR, KWP, CK, AB, LR, TC, RV, MG conceptualized and designed the experiments; JJ, RL,  
362 TC, RV, KS, CL, SReiter, RN, LS, TS, CP, PL, CG, CZ, MH, MT, JR, LZ, SW, BB, KK,  
363 SRamachandran, NP, MÁM-A performed research, TC, RV, KS, CL, KWP, SJR, MG analyzed  
364 data; SJR, KWP, TC, RV, NP, MÁM-A wrote the paper. **Competing interests:** Imanis and  
365 Vyriad authors own options/shares in the companies. This work has been described in one or  
366 more pending provisional patent applications. KWP and SJR are officers of Imanis and Vyriad.  
367 **Data and material availability.** The IMMUNO-COV™ assay is available as a clinically  
368 validated test through a physician order.

369

## 370 **SUPPLEMENTARY MATERIALS**

### 371 **Materials and Methods**

#### 372 **Virus generation and characterization**

373 Full-length human codon-optimized SARS-CoV-2 Spike (S) glycoprotein (NC\_045512.2) in  
374 pUC57 was obtained from GenScript (MC\_0101081). The plasmid was used as a PCR template  
375 to generate a cDNA encoding SARS-CoV-2 spike with a deletion in the nucleotides encoding the  
376 C-terminal 19 amino acids (S- $\Delta$ 19CT) and 5' MluI and 3' NheI restriction sites. To generate the  
377 viral genome, the amplified PCR product containing S- $\Delta$ 19CT was cloned into pVSV in place of  
378 VSV-G using the MluI and NheI restriction sites (Fig. 1). Plasmid was sequence verified and  
379 used for infectious virus rescue on BHK-21 cells as previously described [26]. VSV-G was co-  
380 transfected into the BHK-21 cells to facilitate rescue but was not present in subsequent passages  
381 of the virus. The viruses were amplified and propagated in Vero cells. The amplified viruses do  
382 not have VSV (G) glycoprotein and depend on SARS-CoV-2 spike (S) glycoprotein for entry  
383 and infection. To generate VSV-SARS2(+G), Vero producer cells were electroporated with a  
384 plasmid encoding VSV.G the day before infection with VSV-SARS2. Viruses were harvested  
385 48h post infection and purified prior to use in experiments.

386

387 Correct incorporation of VSV G, N and M proteins and S glycoprotein in virions or virus  
388 infected cells was analyzed by Western blotting using a mouse  $\alpha$ -SARS-CoV-2 Spike (1:1000,  
389 GeneTex #GTX632604), rabbit polyclonal  $\alpha$ -VSV-G antibody (1:20,000, Abcam #ab83196), and  
390 rabbit polyclonal  $\alpha$ -VSV antiserum (1:8000, Imanis #REA-005). Secondary antibodies were  
391 goat  $\alpha$ -mouse IgG-HRP (1:30,000, Prometheus #20-304) and goat  $\alpha$ -rabbit IgG-HRP (1:30,000,  
392 Prometheus #20-303). Membranes were developed for 2 min at room temperature using



393 ProSignal® Dura ECL Reagent (Prometheus #20-301). Protein bands were imaged using a  
394 BioRad ChemiDoc Imaging System. Flow cytometry was performed on infected cells at 8h post  
395 infection. Cells suspensions for flow cytometric analysis were prepared by lifting cells with  
396 Versene solution (Gibco #15040066) followed by staining with a monoclonal antibody against  
397 spike protein conjugated to DyLight™ 633.

398

399 Inhibition of virus infectivity on Vero cells was performed as follows. Vero-DSP1 and Vero-  
400 DSP2 co-monolayers, which produce functional Renilla luciferase following virus-mediated cell  
401 fusion, were seeded at  $6 \times 10^4$  cells per well in 96-well black-walled plates the day before assay.  
402 Neutralizing antibody cocktails were prepared in OptiMEM as follows:  $\alpha$ -SARS-CoV-2 spike  
403 cocktail (mAb10914 at 6  $\mu$ g/mL combined with mAb10922 at 2  $\mu$ g/mL, Genscript) [4],  $\alpha$ -VSV-  
404 G cocktail (mAbVSV-G 8G5F11, Absolute Antibody #Ab01401-2.3) at 2  $\mu$ g/mL combined with  
405 mAb VSV-G IE9F9 (Absolute Antibody #Ab01402-2.0) at 10  $\mu$ g/mL [27], and  $\alpha$ -SARS-CoV-2  
406 spike and  $\alpha$ -VSV-G cocktail (combination of all four antibodies). Three-fold serial dilutions of  
407 the antibody cocktails were prepared and incubated with an equal volume of VSV-SARS2 or  
408 VSV-SARS2(+G). Final antibody concentrations in the virus mixtures were 3  $\mu$ g/mL  
409 mAb10914, 1  $\mu$ g/mL mAb10922 and mAbVSV-G 8G5F11, or 5  $\mu$ g/mL mAbVSV0G IE9F9,  
410 and the final concentration of virus was 200 pfu/100  $\mu$ L. Virus mixed with OptiMEM alone was  
411 used as a control. After a 30 min incubation at room temperature, 100  $\mu$ L of each virus mix was  
412 overlaid onto the Vero-DSP1/2 co-monolayers in duplicate. Plates were returned to a 37°C/5%  
413 CO<sub>2</sub> incubator. After 22 hours, EnduRen™ live cell substrate (6 mM, Promega #E6482) was  
414 added to wells, and luminescence was read after an additional 2 hours using a Tecan M Plex

415 instrument (1000 ms integration, 100 ms settle time per well). Relative luciferase activity  
416 (infection) was determined for each condition relative to the virus in media only control.

417

#### 418 **Nonhuman primate study**

419 **Ethics statement.** This study was conducted as approved by the University of Minnesota  
420 Institutional Animal Care and Use Committee. All animal experiments were executed in an  
421 Association for Assessment and Accreditation of Laboratory Animal Care–approved facility by  
422 qualified staff, following the guidelines and basic principles in the National Institutes of Health  
423 (NIH) Guide for the Care and Use of Laboratory Animals [28], the Animal Welfare Act, the U.S.  
424 Department of Agriculture, and the U.S. Public Health Service Policy on Humane Care and Use  
425 of Laboratory Animals. The University of Minnesota Institutional Biosafety Committee (IBC)  
426 approved work with VSV strains under BSL2 conditions and was performed according to IBC-  
427 approved standard operating procedures.

428

429 **Animals.** Twenty-two adult male and female adult Mauritian origin cynomolgus macaques  
430 (*Macaca fascicularis*) were allocated for this study. They were socially housed in same sex pairs  
431 or groups in climate-controlled rooms with a fixed light-dark cycle (12/12 hours) with a 30  
432 minute sunrise illumination and sundown fade. Commercial monkey chow, 2055C Teklad  
433 Global Certified 25% Protein Primate Diet from Harlan Laboratories, and fruits or vegetables  
434 were provided twice daily and water was available ad libitum. The behavioral management  
435 program included social housing in pairs (except during bond breakdown or pending  
436 reintroduction), enrichment, and basic training. Environmental enrichment included human  
437 interaction and a variety of treats, toys, foraging puzzles, and sensory stimuli like music.

438 Structural enrichment included perches, swings, and climbing apparatus. NHPs were trained  
439 prior to study for cooperation with routine husbandry tasks only which included targeting and  
440 shifting [29, 30].

441  
442 In experiment 1, eighteen adult males and females with the median age of 3.7 years (range 3.4 to  
443 6.7 years) and median body weight of 4.8 kg (3.2 to 6.8kg) were stratified by sex and randomly  
444 assigned to control and vaccine groups (Fig. 2). Animals received Sham control (N=6) at an  
445 equivalent volume to vaccinated animals, animals in vaccine groups received VSV-SARS2 at a  
446 dose of  $10^7$  TCID<sub>50</sub> PO (N=6) or  $10^7$  TCID<sub>50</sub> IM (N=6) on day 0. All 12 vaccinated animals  
447 received an oral dose of VSV-SARS2(+G) as an oral boost on day +42. In experiment 2, four  
448 demographically similar males with median age of 4.4 years (range 4.4 to 5.2 years) and median  
449 weight of 5.5kg (range 5.1 to 6.1 kg) were used (Fig. 3). Animals received VSV-SARS2(+G) at a  
450 dose of  $10^8$  TCID<sub>50</sub> PO (N=2) or IM (N=2) on day 0. Intramuscular vaccines were administered  
451 with a needle and syringe without adjuvant or orally using an oral syringe and gently tipping the  
452 head slightly back to deliver under the tongue and into the cheek pouches, with gently swabbing  
453 around the mouth with a cotton swab during the 5 minute dwell to mimic swishing.

454  
455 **Safety evaluation.** Clinical observations of animals were performed at least twice daily for  
456 general attitude, activity level, gait, posture, appearance, feces, urine and any signs of pain or  
457 distress. Body weight was measured at least weekly. Animals were sedated for sham or test  
458 article administration, blood collection, and clinical exams using ketamine (5-15mg/kg IM) and  
459 midazolam was added (0.1-0.3mg/kg IM), if necessary, to extend sedation. All exams included  
460 weight and temperature measurements, complete examination of the oral mucosa, swabs, and

461 blood sampling. Blood was collected using a peripheral vein and standard catheter at  
462 qualification, baseline prior to vaccination, then post vaccination biweekly, weekly, monthly or  
463 bi-monthly based on phase for clinical pathology that included complete blood counts, blood  
464 chemistries, CRP, and coagulation profiles. At these same timepoints nasal, buccal, and rectal  
465 swabs and fresh stool were also collected. At selected timepoints, additional assessment of  
466 immune profile pre and post vaccination was performed that included neutralizing antibody  
467 response and CD4/CD8 T cell response and characterization of VSV viremia and viral shedding.

468

469 **Study Termination.** All animals were euthanized at the completion of study and a full necropsy  
470 was performed which included a full gross examination. Bronchial alveolar lavage (BAL) was  
471 performed at necropsy by insertion of tube into the trachea, past the third bifurcation, and  
472 subsequent installation of 5-10 ml of sterile saline. Manual suction was applied to retrieve the  
473 BAL sample. Harvested tissues were fixed for a minimum of 72 hours in 10% neutral-buffered  
474 formalin and then embedded in paraffin. These tissues were evaluated histologically for signs of  
475 pathology by a board-certified veterinary pathologist blinded to study group allocations.

476

#### 477 **NHP Antigen Binding ELISA against SARS-CoV-2 Spike Trimer**

478 Nunc Maxisorp microtiter plates (ThermoFisher Scientific) were coated with 100 ng/well of  
479 recombinant SARS-CoV-2 spike trimer protein (Cat.# SPN-C52H2, Acro Biosystems) in  
480 200mM carbonate-bicarbonate buffer, pH 9.4. overnight at 4°C. Plates were washed and blocked  
481 with 1× SuperBlock™ in PBS for 30 minutes at room temperature (RT). Plates were washed  
482 again and incubated with serial dilutions of NHP sera or bronchiolar lavage fluid (BALF) diluted  
483 in sample buffer (1× SuperBlock™ T20 in PBS) and incubated for 90 minutes at RT. Plates were

484 washed three times with PBS with 0.05% Tween 20 and then incubated for 45 minutes at RT  
485 with either horse radish peroxidase (HRP)- conjugated anti-NHP IgG (1:10,000, Cat.# PA1-  
486 84631, Invitrogen) or HRP-conjugated anti-NHP IgA (1:5,000, Cat.# 5220-0332, SeraCare)  
487 secondary antibodies diluted in sample buffer. After a final washing step, plates were developed  
488 using 100µl of SureBlue™ 1-Step TMB Substrate (3,3',5,5'-tetramethylbenzidine; SeraCare)  
489 and the reaction stopped with an 100µL volume of HCl TMB Stop Solution (SeraCare) before  
490 the optical density (OD) was read at 450nm with a 630nm reference wavelength nm using an  
491 Infinite M200Pro microplate reader (Tecan). The dilution titers from serum IgG were  
492 determined using a cut point established for each animal based on Day 0 serum collection  
493 (collected prior to vaccination) and then multiplied by a cut point factor. For analysis of BALF  
494 IgA, the cut point was obtained using the average signal of the control group animals multiplied  
495 by a cut point factor. Cut point factors were determined separately for each antibody type and  
496 matrix using 95% confidence intervals obtained from individual analyses of the seronegative  
497 samples (pre-immune or saline control animals, respectively). Pre-immune serum paired to each  
498 animal was included on each analytical run to establish the plate-specific cut point on each assay  
499 plate. Dilution titers were calculated by fitting the data of all dilutions of a sample with a 4-  
500 parameter logistic curve to determine the dilution where absorbance signal falls below the cut  
501 point. Due to limited sample volume in evaluating IgA from the buccal swabs, the raw OD450  
502 (with subtraction of 630nm reference) was compared directly between swab preparations  
503 prepared from saline control animals with swab preparations prepared from animals that received  
504 the oral VSV-SARS2(+G) boost.

505

506 **IMMUNO-COV™ Neutralization Assays of NHP Samples**

507 Vero-ACE2 cells were seeded at  $10^4$  cells/well in 96-well black-walled plates with clear bottoms  
508 16-24 h before being used for neutralization assays. On the day of assay, increasing dilutions  
509 (1:80, 1:160, 1:320, 1:640, 1:1280, and 1:2560) of serum samples were prepared and mixed with  
510 VSV-SARS2-Fluc in U-bottom suspension cell culture plates to a final volume of 240  $\mu$ L/well.  
511 Virus, test samples, and controls were all diluted as appropriate in OptiMEM to generate final  
512 concentrations. Serum dilutions represent the final dilution following mix with virus. Virus was  
513 used at 300 pfu/assay well (300 pfu/100  $\mu$ L in U-well mixtures). Pooled seronegative NHP  
514 serum was used as a negative control, and pooled seronegative NHP serum spiked with  
515 monoclonal anti-SARS-CoV-2 spike antibody was used as a positive control. Virus mixes in U-  
516 well plates were incubated at room temperature for 30-45 min, and then 100  $\mu$ L of mixes were  
517 overlaid onto the Vero-ACE2 monolayers in duplicate. All time points for each animal were  
518 assayed on the same plate. Plates were returned to a 37°C/5% CO<sub>2</sub> incubator for 24-28 hours. D-  
519 luciferin was then added to wells and luminescence was read immediately (30-90 seconds) using  
520 a Tecan M Plex or Tecan Lume instrument (100 ms integration, 100 ms settle time per well).  
521 Virus neutralizing titers were determined for each sample from an individual animal by  
522 calculating the dilution that resulted in luciferase signal greater than 50% of the Day 0 (prior to  
523 treatment) sample for that specific animal (IC<sub>50</sub>). The dilution was calculated by fitting all  
524 dilutions to a 4-parameter logistic curve fitting model.

525

### 526 **VSV-G Antibody Neutralization Assays of NHP Samples**

527 NHP serum samples and positive control rabbit  $\alpha$ -VSV antiserum (Imanis #REA-005) were heat  
528 inactivated at 56°C for 30 min. Two-fold serial dilutions of samples and positive controls were  
529 prepared in quadruplicate starting at 1:10. Dilutions were mixed with equal volumes of VSV-

530 GFP, such that the final VSV-GFP concentration was 400 TCID<sub>50</sub>/100 µL and the final serum  
531 and positive control concentrations were 1:20, 1:40, 1:80, 1:160, 1:320, 1:640, 1:1280, 1:2560,  
532 1:5120, 1:10240, and 1:20480. Virus mixed with media alone was used as a negative control.  
533 After a 1 hour incubation at 37°C, 2×10<sup>4</sup> BHK-21 cells were overlaid onto the virus mixes. Plates  
534 were incubated at 37°C/5% CO<sub>2</sub> for 48 hours, at which time each well was scored for the  
535 presence or absence of cytopathic effects (CPE; cell death).

536

### 537 **Infectious Virus Recovery (IVR) Assays**

538 Buccal, rectal, and nasal swabs were cut and placed in 700 µL of OptiMEM containing  
539 antibiotics. After a 1 min. vortex at maximum speed, swabs were snap frozen in liquid nitrogen  
540 and then thawed at room temperature. Samples were centrifuged at 12,000 x g for 5 minutes at  
541 4°C, then filtered through a 0.22 µm syringe filter. Testing of swab samples spiked with VSV-  
542 ΔG-SARS-CoV-2-S indicated that this method of virus extraction was compatible with recovery  
543 of infectious virus from swabs. Ten-fold serial dilutions starting at 10<sup>-1</sup> of the samples were  
544 overlaid onto monolayers of Vero-αHis cells plated the day before. VSV-SARS-CoV-2-S-  
545 Δ19CT [17] was used as a control. Plates were incubated at 37°C/5% CO<sub>2</sub> for 24 hours, at which  
546 time media was aspirated from all wells. Wells were washed with OptiMEM and then 100 µL of  
547 OptiMEM with 0.0004% trypsin/EDTA was added to each well. Plates were incubated for an  
548 additional 3 days at 37°C/5% CO<sub>2</sub> before each well was scored for the presence of syncytia,  
549 indicative of infectious virus. Remaining preparations from buccal swabs prepared for IVR were  
550 used to evaluate NHP IgA against SARS-CoV-2 spike trimer in a binding ELISA assay.

551

### 552 **Mice study**

553 All animal procedures were reviewed and approved by the Mayo Clinic Institutional Animal  
554 Care and Use Committee. Female and male Ifnarm-CD46Ge mice [31] received intra-  
555 peritoneally  $5 \times 10^5$  TCID<sub>50</sub> virus particles or 5 $\mu$ g of SARS-CoV-2 spike protein (Cat.# V0589-  
556 V08B, Sino Biological) adjuvanted with aluminum (Cat.#vac-alu-250,InvivoGen) on day 0 and  
557 21. On days 21 (before boost) and 41, blood was collected. Parallel groups of mice were  
558 terminated on day 21 post-immunization for analysis of cellular immune response.

559

### 560 **Mouse Antigen binding ELISA**

561 Nunc ELISAs plates (ThermoFisher Scientific) were coated with 100 ng of recombinant SARS-  
562 CoV-2 spike protein (Cat.# V0589-V08B, Sino Biological) in 50mM carbonate-bicarbonate  
563 buffer, pH 9.6. overnight at 4°C. Plates were washed and blocked with 2% bovine serum  
564 albumin (BSA) in PBS for 2h at room temperature (RT). Plates were washed again and incubated  
565 with serial dilutions of mouse sera and incubated for 1h at 37°C. Plates were washed three times  
566 with PBS with 0.05% Tween 20 and then incubated for 1h at RT with horse radish peroxidase  
567 (HRP)- conjugated anti-mouse IgG (1:5,000, Cat.#62-6520, ThermoFisher Scientific) , IgG1  
568 (1:5,000, Cat.# 115-035-205, Jackson ImmunoResearch) or IgG2a (1:5,000, Cat.# 115-035-206,  
569 Jackson ImmunoResearch) secondary antibody. After final wash, plates were developed using  
570 50 $\mu$ l of 1-Step Ultra TMB (3,3',5,5'-tetramethylbenzidine; ThermoFisher Scientific) and the  
571 reaction stopped with an equal volume of 2M sulfuric acid before the optical density (OD) was  
572 read at 405 nm using an Infinite M200Pro microplate reader (Tecan). The endpoint titers of  
573 serum IgG responses were determined as the dilution that emitted an optimal density exceeding  
574 average of OD values plus three standard deviations of negative serum samples.

575



576 **Pseudovirus production and neutralization assay**

577 Pseudotyped lentiviruses with the SARS-CoV-2 spike protein were produced as described  
578 elsewhere [32]. In brief, HEK293T cells seeded overnight were transfected with HDM-Hgpm2,  
579 HDM-tat1b, pRC-CMV-Rev1b, pHAGE-CMV-Luc2-IRES-ZsGreen-W and a codon-optimized  
580 SARS-CoV-2 spike encoding the D614G amino acid change. The culture media was changed to  
581 fresh media containing antibiotics 18h to 24h post-transfection. At 60h post-transfection,  
582 supernatants were harvested and passed through a 0.45µm filter. For pseudovirus neutralization  
583 assay, three-fold serially diluted serum samples were mixed with SARS-CoV-2-pseudotyped-  
584 lentiviruses for 1 hours at 37 °C. And the mixture was added in quadruplicates to hACE-2-  
585 expressing HEK293T cells overnight, followed by media replenishment. At 60-72 hours-post  
586 incubation, the luciferase activity was detected by Bright-Glo Luciferase assay system (Cat.#  
587 E2610, Promega, Madison, WI, USA). The percentage of infection was calculated as the ratio of  
588 luciferase value with antibodies to that without antibodies. The half maximal inhibitory  
589 concentration (IC50) was determined by non-linear regression using GraphPad Prism version  
590 8.4.2 for macOS (GraphPad Software, San Diego, CA, USA).

591

592 **ELISpot Analysis**

593 Frozen PBMCs were used to evaluate IFN $\gamma$ , IL-4 T cell responses in NHP and frozen  
594 splenocytes were used IFN $\gamma$  T cell responses in murine samples. Individual overlapping SARS  
595 CoV-2 Spike peptides (BEI Resources, NIAID, NIH: Peptide Array, SARS-Related Coronavirus  
596 2 Spike (S) Glycoprotein, NR-52402; S1: 1 to 97 peptides, S2: 98 to 181 peptides), were pooled  
597 and dissolved in DMSO. Peptides were used at 0.5ug/ml concentration per peptide to elicit IFN $\gamma$   
598 and/or IL-4 responses. For NHP samples, low-fluorescent PVDF membrane (Millipore, Bedford,

599 MA, USA) plates were coated with IFN $\gamma$  and IL-4 capture antibodies overnight. Previously  
600 frozen PBMCs from NHP were washed, resuspended in T cell media (RPMI 1640 media  
601 containing 25 mM HEPES, NEAA, 2 mM L-glutamine, 1 mM sodium pyruvate, 0.05mM 2-  
602 mercaptoethanol supplemented with 10% (vol./vol.) heat-inactivated fetal bovine serum),  
603 counted and added to wells at 250,000 cells per well. SARS CoV2 Spike domain peptide pools  
604 (S1 and S2) were added to the plate and incubated at 37°C for 48 hours. Media containing  
605 equivalent DMSO and PMA/I were used as negative and positive controls respectively. Plates  
606 were then developed as per manufacturer's instructions (MabTech Inc). Spot forming cells (SFC)  
607 were counted using automated MabTech IRIS reader with excitation/emission of 490nm/510nm  
608 for IFN $\gamma$  and 550nm/570nm for IL-4.

609

610 For murine samples, ELISpot assays were performed using the mouse IFN-gamma ELISpot kit  
611 (Cat.# EL485, R&D systems Briefly,  $5 \times 10^5$  isolated splenocytes were added along with different  
612 stimuli in 200  $\mu$ l of RPMI 1640 medium supplemented with 10% (vol./vol.) heat-inactivated  
613 fetal bovine serum for 48 h on each well of IFN- $\gamma$  coated plates. Pooled 15-mer overlapping  
614 peptides from SARS-CoV-2 spike glycoprotein (BEI Resources) were used to stimulate  
615 splenocytes at 0.1 $\mu$ g of individual peptides/ml. As a positive control, PMA/Ionomycin cell  
616 stimulation cocktail (Biolegend, USA) was used at 2.5 $\mu$ l/ml, and as negative control, splenocytes  
617 were stimulated with equivalent DMSO concentration (0.8%). Post 48-hour incubation, plates  
618 were developed in accordance with manufacturer instructions. Developed IFN- $\gamma$  spots were  
619 counted with an automated ELISPOT reader (CTL Analyzers LLC, USA). Each spot represented  
620 a single reactive IFN- $\gamma$ -secreting T cell. Spots were normalized to DMSO control and figures  
621 represented as SFC per million cells for S1 and S2 peptide pools combined.

622

623 **Statistical analyses**

624 Tukey's multiple comparison test or a two-tailed unpaired Student's t test was conducted to  
625 compare differences between vaccine groups and the control group with Bonferroni correction  
626 applied to control the type I error rate for the comparisons.

627

628

629 **Figure Legends**

630 **Figure 1: Generation and characterization of VSV-SARS2 and VSV-SARS2(+G) viruses.**

631 (A) Schematic of the VSV-SARS2 genome and nomenclature of viruses. (B) Crystal violet  
632 stained A549 cells and A549-ACE2 cells at 24h after virus infection. Note the extensive  
633 syncytial formation in the VSV-SARS2 and VSV-SARS2(G) infected A549-ACE2 expressing  
634 cells. (C) Immunoblot of virions prepared in untransfected or G-plasmid transfected Vero cells,  
635 and of lysates from corresponding virus infected cells were probed with polyclonal VSV  
636 antiserum and a monoclonal antibody against the S2 domain of the SARS-CoV-2 spike  
637 glycoprotein. The S2 shadow band in the cell lysates may be a glycosylation variant. (D) Flow  
638 cytometry analysis of anti-spike stained virus infected cells. (E) Neutralization of the infectivity  
639 VSV-SARS2 (+/- G) by a cocktail of anti-G and/or anti-S monoclonal antibodies.

640

641 **Figure 2: VSV-SARS2 is poorly immunogenic in cynomolgus macaques (IM and oral**  
642 **routes).**

643 (A). Experimental design showing groups of six cynomolgus macaques vaccinated by  
644 intramuscular (IM) or oral (PO) routes using  $10^7$  TCID<sub>50</sub> VSV-SARS2 virus. Another six  
645 animals received vehicle control via both IM and PO routes. Baseline and post-vaccination  
646 samples were harvested at indicated timepoints. (B) IgG anti-spike antibody titers by ELISA. (C)  
647 Neutralizing antibody titers using a live SARS-CoV-2 spike VSV pseudovirus (IMMUNO-  
648 COV™) assay [17]. Time points are before (pre) and at 2, 3, and 4 weeks post vaccination. A  
649 log<sub>2</sub> scale is used for the y axis.

650

651 **Figure 3: VSV-SARS2(+G) is powerfully immunogenic in cynomolgus macaques.** 4 NHP  
652 were given the VSV-SARS(+G) vaccine by IM (IM-1, IM-2) or PO routes (PO-1, PO-2). Titers

653 of anti-spike (A) IgG and (B) neutralizing antibodies against a live SARS-CoV-2 spike  
654 pseudovirus were measured at various time points. (C) Anti-VSV.G IgG titers in the orally or IM  
655 vaccinated animals. (D) Th1 (IFN-gamma secreting) and Th2 (IL-4 secreting) ELISPOT assay  
656 for spike antigen reactive T cells in peripheral blood mononuclear cells (PBMC) at day 42.

657

658 **Figure 4: Oral VSV-SARS2(+G) powerfully boosts the immune response in vaccine-primed**

659 **cynomolgus macaques.** (A) Experimental design. Animals received initial VSV-SARS2 vaccine

660 by IM or PO routes, and at day 42, the IM vaccinated NHP received an oral boost of VSV-

661 SARS2(+G). 4 NHP received the high dose of  $10^9$  TCID<sub>50</sub> and 2 NHP received the lower dose of

662  $5 \times 10^6$  TCID<sub>50</sub> VSV-SARS2(+G) (B) IgG titers against spike. (C) Neutralizing antibody titers

663 using the live SARS-CoV-2 spike VSV pseudovirus and (D) a lentiviral pseudovector displaying

664 the spike protein. (E) IFN-gamma and IL-4 ELISPOT assay for spike antigen reactive T cells

665 from peripheral blood mononuclear cells (PBMC) after oral boost with VSV-SARS2(+G). G=

666 VSV-SARS(+G) virus, S=VSV-SARS2 virus (F) Anti-VSV.G IgG antibody titers in boosted

667 animals. (G) Anti-spike IgA titers in bronchoalveolar lavage fluid (BALF) and (H) buccal fluid

668 of animals.

669

670

671

672

673

674

675

676

677

678

679

## 680 **Supplemental Figure Legends**

681 **Supplemental Figure 1: VSV-SARS2(+G) is powerfully immunogenic in mice.** (A) Ifnartm-  
682 CD46Ge mice were vaccinated on day 0 and 21 with VSV-SARS2(+G) or irrelevant virus  
683 (control). Sera was collected on day 21 and 41. Spleens from vaccinated mice were collected  
684 from parallel groups. Collected sera were assessed by ELISA for SARS-CoV-2 spike-specific  
685 IgG (B), IgG1 and IgG2a (C). End-point titers (B) and end-point titer ratio of IgG1 to IgG2a (C)  
686 were calculated. Serum samples from animals immunized with SARS-CoV-2-Spike adjuvanted  
687 with Alum were used as control for a TH<sub>2</sub> biased response. Pseudovirus neutralizing antibody  
688 responses were also calculated in vaccinated animals (D). In (E), splenocytes were isolated and  
689 stimulated with vehicle (media), PMA, or pools of overlapping peptides from SARS-CoV-2  
690 spike. The number of cells expressing IFN- $\gamma$  per 10<sup>6</sup> splenocytes is displayed. Dots represent  
691 individual animals. Horizontal bars are mean per group.

692

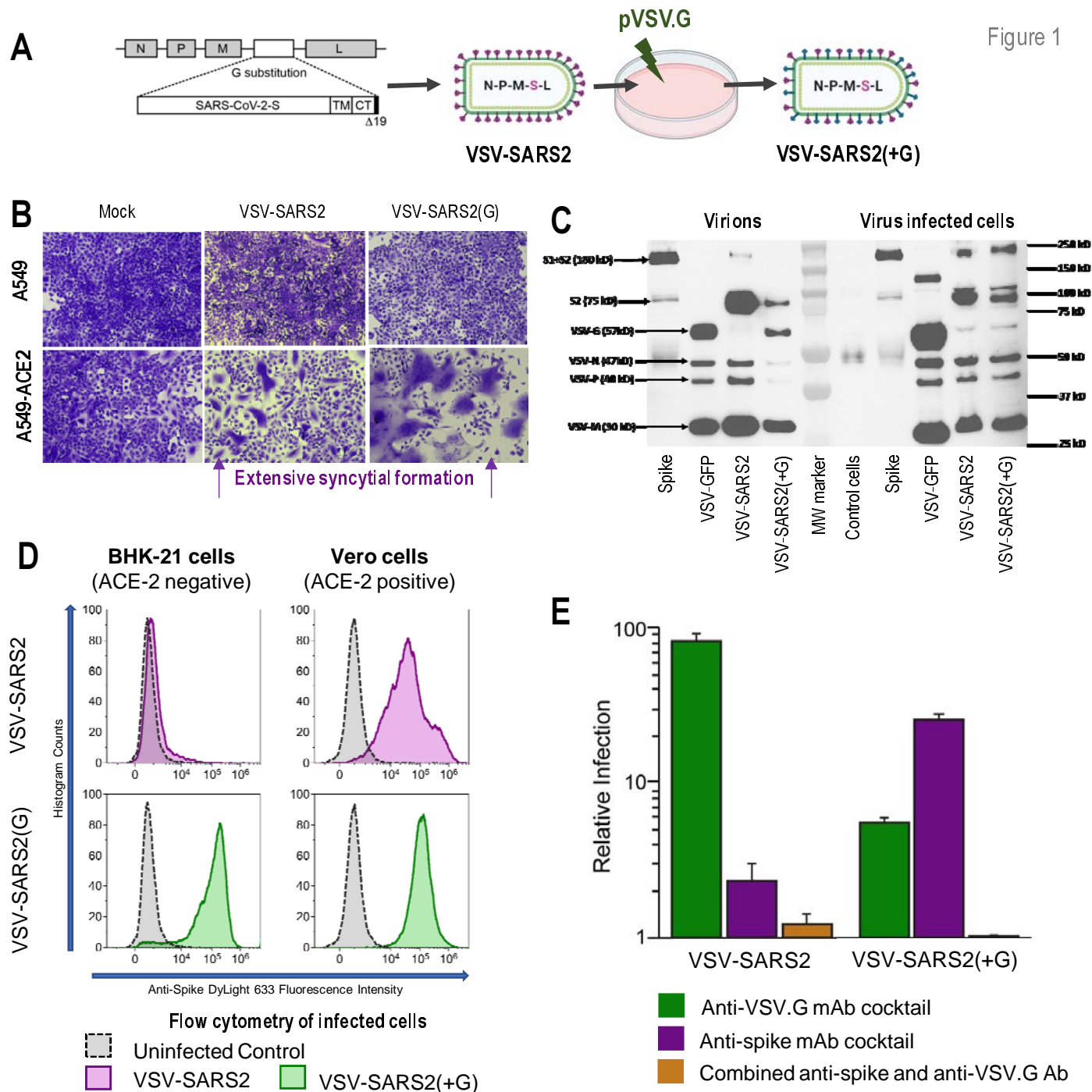
693 **Supplemental Figure 2.** Good correlation in neutralizing antibody titers (nAb) measured using  
694 IMMUNO-COV assay that uses a VSV based versus a lentiviral based pseudovirus.

695

696 **Supplemental Figure 3.** (A) Body weights, (B) temperature and (C) serum c-reactive protein in  
697 NHP after one prime dose of VSV-SARS(2) on day 0, and an oral boost of VSV-SARS2(+G) at  
698 day 42.

699

Figure 1



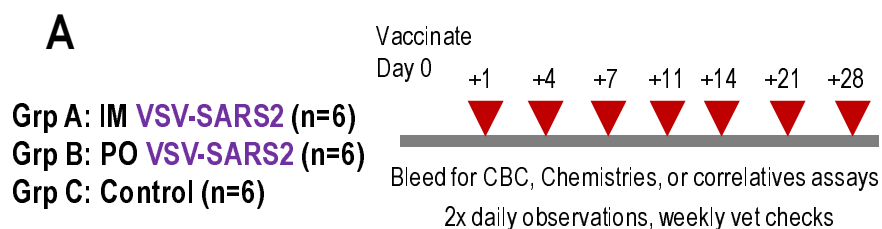


Figure 2

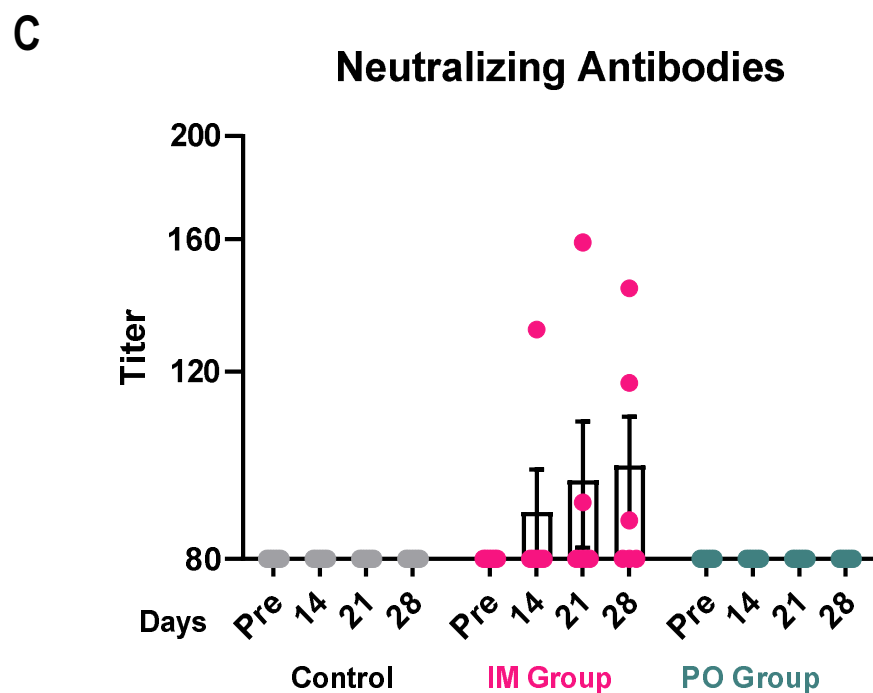
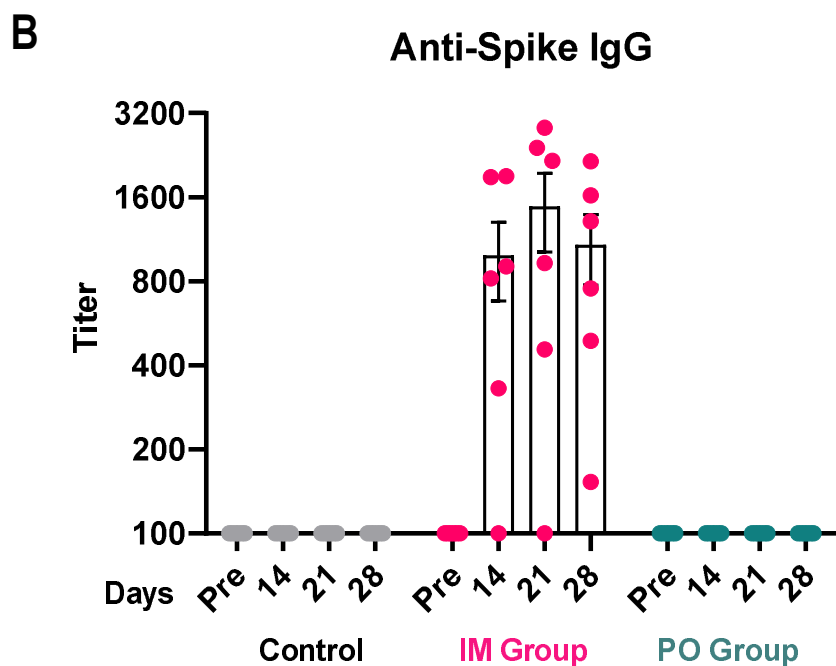




Figure 3

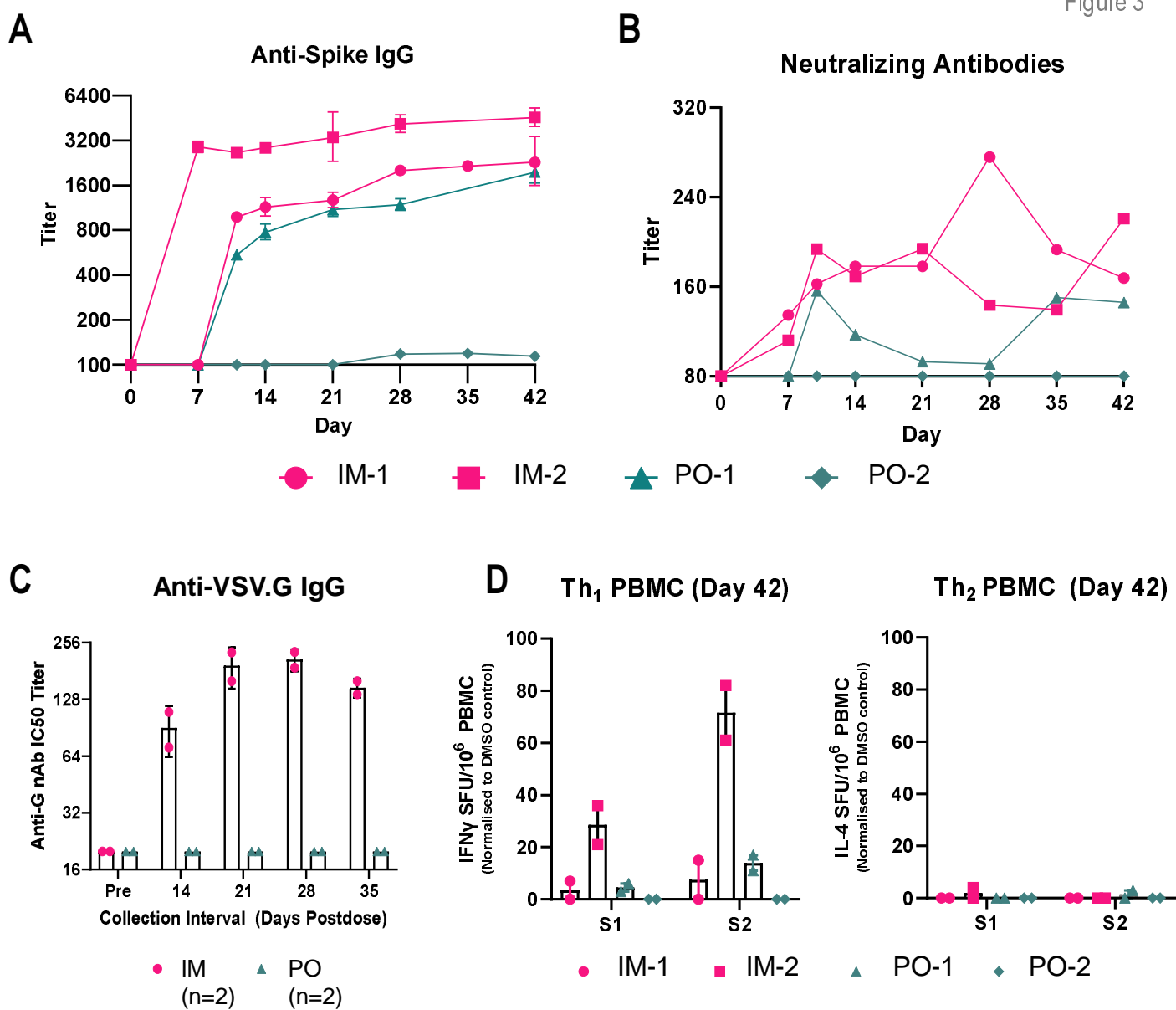
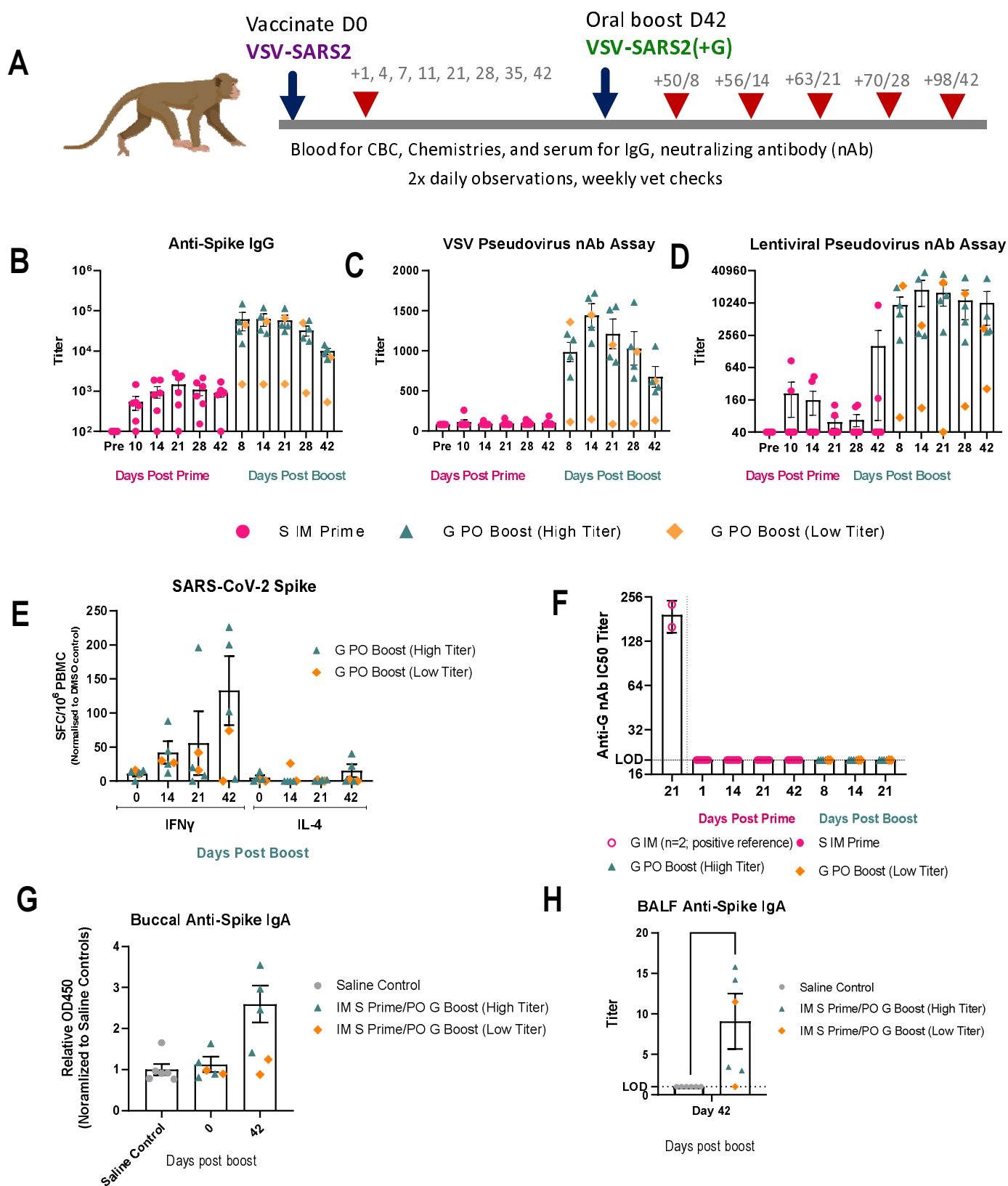
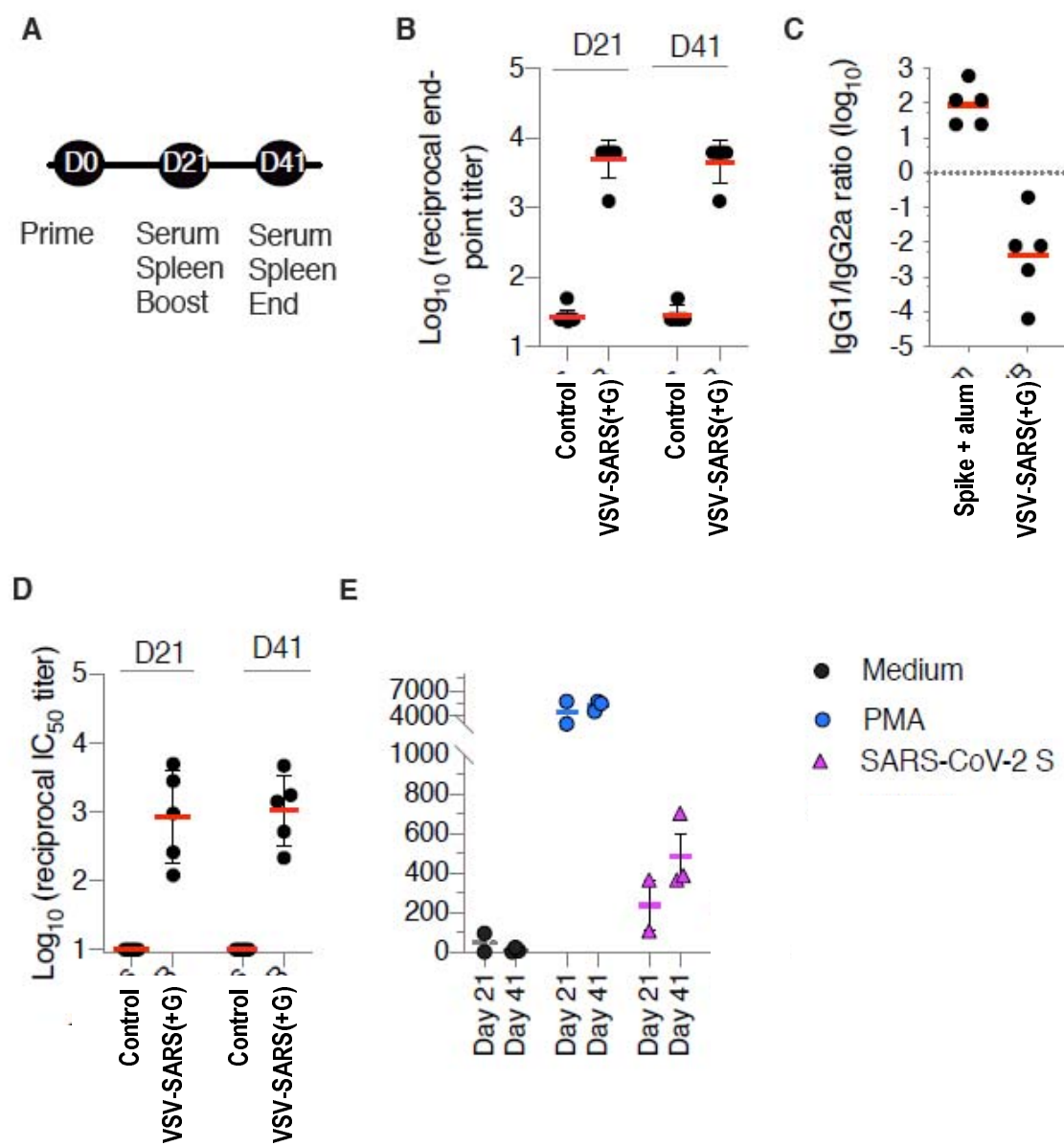
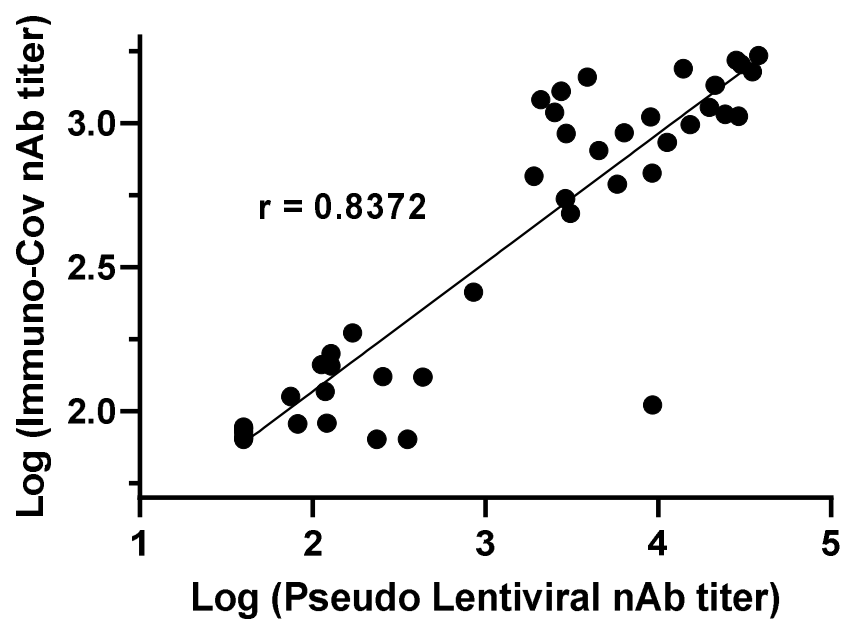


Figure 4

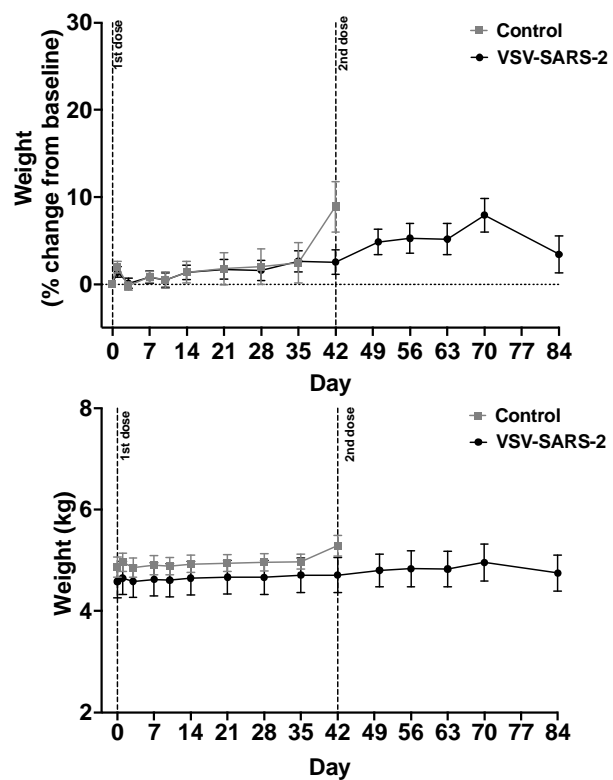


Supplemental figure 1

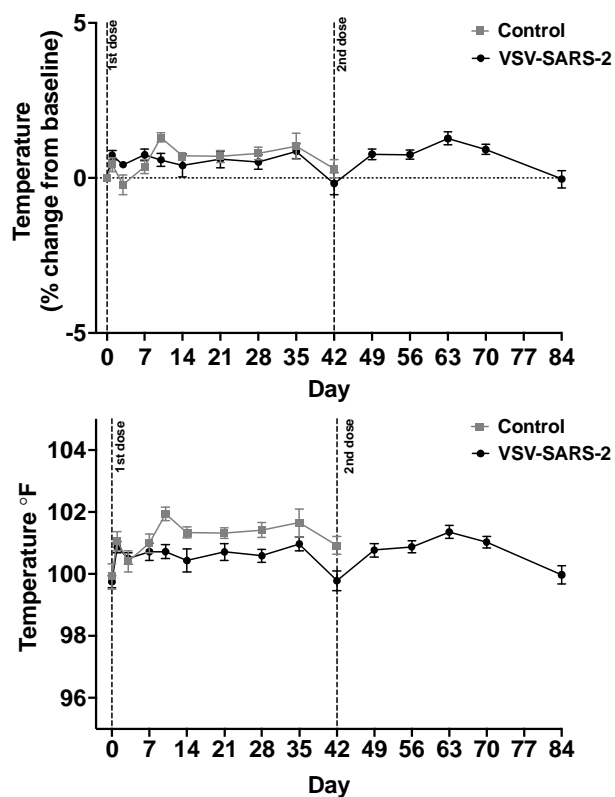




### A. Body weight



### B. Body temperature



### C. C-reactive protein

